A density functional model for the surface properties of liquid ^{4}He

1992 J. Phys.: Condens. Matter 4 667

(http://iopscience.iop.org/0953-8984/4/3/008)

J. Phys.: Condens. Matter 4 (1992) 667–678. Printed in the UK

A density functional model for the surface properties of liquid ^{4}He

A Guirao, M Centelles, M Barranco, M Pi, A Polls and X Viñas
Departament d'Estructura i Constituents de la Matèria, Facultat de Física, Universitat de Barcelona, Diagonal 647, E-08028 Barcelona, Spain

Received 25 July 1991

Abstract. A density functional approach is proposed to study the ^{4}He liquid–gas interface. The free energy density, which depends on the particle density and temperature, has been adjusted to reproduce the liquid density and the vapour pressure along the liquid–gas coexistence line, as well as the zero-temperature surface tension. After achieving a fairly good description of the phase transition, the calculated surface tension agrees well with the experimental results. The calculated density profile is used to discuss a recent experimental determination of the surface thickness.

1. Introduction

The surface tension (σ) of liquid ^{4}He was first measured in 1925 [1]. However, there still are many open theoretical and experimental problems in the description of the liquid–gas interface [2]. It is only recently that the surface tension of liquid ^{4}He has been systematically measured from the critical temperature T_c down to a few tenths of kelvin [3, 4]. Apart from the surface tension, the experimental information on the liquid–gas interface is very scarce; only a few indirect determinations of the surface thickness (t) are available [5, 6]. The analysis of the most recent experiments, which are based on ellipsometric measurements, [6] requires the knowledge of the density profile $\rho(z)$. As there is not enough experimental information on $\rho(z)$, it is necessary to guess a density profile, which in [6] was chosen to be a simple Fermi function.

At zero temperature (T), there exist in the recent literature different theoretical methods to study the free surface of liquid ^{4}He. Basically, they fall into one of two types, namely microscopic [7–9] and phenomenological [10, 11] models. In the first type, the extensions of the variational Monte Carlo and Green's function Monte Carlo methods to inhomogeneous systems [9] predict a surface tension in very good agreement with the experimental results. The second type of calculations is based mainly on density functional theories which have received a renewed interest in their application to quantum liquids [10–14] and will constitute the framework of the present investigation.

The situation at finite temperature is more complicated and to our knowledge there is no microscopic calculation of the liquid–gas interface. In fact, the very few microscopic attempts to describe ^{4}He at $T \neq 0$ have been concentrated in the bulk properties [15, 16]. It is precisely in these situations where a more phenomenological approach, such as a density functional theory, can be useful to analyze the experimental results.

0953-8984/92/030667+12$03.50

Recently, simple energy density functionals have been used with some success to study the ^{3}He liquid–gas interface at non-zero temperatures [14,17]. These functionals were largely inspired on the density functional proposed in [10] to study liquid helium at $T = 0$. In this reference, Stringari and Treiner achieved a good description of the $T = 0$ K liquid equation of state and of the properties of the free surface, once the few parameters entering the functional definition had been chosen to reproduce some relevant, experimentally known quantities.

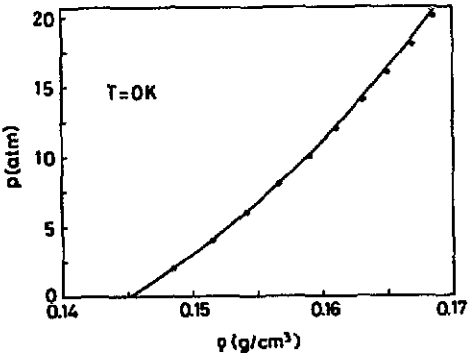

Figure 1. ^{4}He $T = 0$ K isotherm. The full circles are the experimental values from [20].

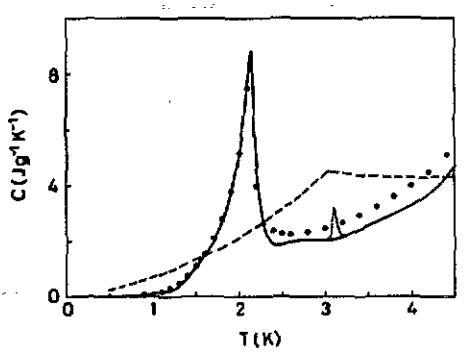

Figure 2. Liquid specific heat along the coexistence line. The full circles are the experimental values from [20]. The broken curve corresponds to the specific heat of a free Bose system at the same density and temperature.

It is the purpose of this paper to present an extension to finite temperatures of the ^{4}He density functional formalism of [10] in order to study the T-dependence of the liquid–gas interface properties. Any attempt to accurately describe the ^{4}He surface properties should start from a proper description of the homogeneus system and of the liquid–gas equilibrium as well. The simplest extension to $T \neq 0$ of the formalism of [10] is the thermal Hartree approximation. As it will be seen in section 2, this approach yields results only in qualitative agreement with experiment. To describe the liquid–gas equilibrium in a quantitative way, we will go a step further and construct a free energy density $F(\rho, T)$ depending on the particle density ρ and the temperature T. At each value of T, the parameters entering the functional have been fitted to reproduce the vapour pressure and liquid density along the liquid–gas coexistence line, thus introducing a temperature dependence in the coefficients. A similar procedure has been used with some success for liquid ^{3}He [14].

This paper is organized as follows. In section 2 we construct the density functional for the bulk and analyze its capability to study the liquid–gas equilibrium. Secion 3 is devoted to discuss the interface properties at $T \neq 0$. To this end, the bulk density functional is completed by adding terms that account for density inhomogeneities. The surface tension and the density profiles are calculated and used to analyze the experimental results of [6]. Finally, a short summary is presented in section 4.

2. Liquid–gas equilibrium

An appropriate thermodynamic potential to study the behaviour of the system is the

free energy density

$$F(\rho,T) = h(\rho,T) - Ts(\rho,T) \tag{1}$$

where h and s are the energy and entropy densities per unit volume respectively. It is convenient to write the functional (1) in the following form:

$$F(\rho,T) = f_{ni}(\rho,T) + f_v(\rho,T)\,. \tag{2}$$

$f_{ni}(\rho,T)$ is the free energy density of a non-interacting Bose gas [18] and $f_v(\rho,T)$ is the contribution due to the interatomic interaction. This quantity can be evaluated using an effective interaction in the context of a mean field approach, as for example the Hartree method for Bose systems. An especially simple result is obtained using a local zero range interaction. In this case f_v is T-independent. In particular, the use of the local Skyrme-type interaction proposed in [10] at $T = 0$, yields the following expression for f_v:

$$f_v(\rho,T) = \tfrac{1}{2}b\rho^2 + \tfrac{1}{2}c\rho^{2+\gamma}\,. \tag{3}$$

In this model, the first term originates from an attractive two-body contact force, while the second term comes from a repulsive density-dependent interaction, such a dependence being characterized by the parameter γ. At $T = 0$, there is no contribution from $f_{ni}(\rho,T)$ and the free energy density reduces to f_v. The parameters b, c and γ have been fixed so as to reproduce, at saturation, the experimental density ($\rho_0 = 0.02184$ part Å^{-3}), binding energy ($e_0 = -7.17$ K) and incompressibility ($\kappa = 0.597$ K Å^{-3}) defined as

$$\kappa = \rho\left(\frac{\partial p}{\partial \rho}\right)_T \tag{4}$$

where p is the pressure. The fit of these experimental quantities yields $b = -890.215$ K Å^3, $c = 1.0960 \times 10^7$ K (Å^3)$^{1+\gamma}$ and $\gamma = 2.813$. The isotherm at $T = 0$ is shown in figure 1 together with the experimental points. One can see that the agreement is satisfactory up to pressures close to the solidification pressure.

Although the expression for $f_{ni}(\rho,T)$ at $T \neq 0$ is given in textbooks [18] we include here a brief summary of its derivation to illustrate the strategy of the method. At each T, we define ρ_e as

$$\rho_e(T) = \frac{1}{2\pi^2}\left(\frac{2mT}{\hbar^2}\right)^{3/2} C_{1/2}(0) \tag{5}$$

where

$$C_\nu(\eta) = \int_0^\infty \mathrm{d}x \frac{x^\nu}{e^{x-\eta}-1}\,. \tag{6}$$

The value of $\hbar^2/m$ for a ^{4}He atom is 12.119 K Å^2 and η is the degeneracy parameter. For a free Bose gas, $\eta = \mu/T$, where μ is the chemical potential, and $\eta = (\mu - \partial f_v/\partial\rho)/T$ if the particles are submitted to a single-particle (SP) mean field $\partial f_v/\partial\rho$.

ρ_e is the maximum density which, in this mean field approximation, the Bose system can accomodate in non zero momentum SP states. For $\rho > \rho_e$, a Bose–Einstein condensation takes place and a fraction of $(\rho - \rho_e)/\rho$ particles occupies the zero momentum state. This occurs when $\eta = 0$, and equation (5) defines the so-called lambda line in the $\rho - T$ plane. This line intersects the liquid branch of the liquid–gas equilibrium diagram at a point called the lambda point which corresponds to a temperature T_λ. For the above parameterization, $T_\lambda = 3.2$ K. The lambda point manifests itself as a discontinuity in the T-derivative of the specific heat along the liquid–gas coexistence line, see the broken curve in figure 2. We shall come back to this point later on.

To find η for $\rho < \rho_e$, it is necessary to solve the following implicit equation:

$$\rho = \frac{1}{2\pi^2}\left(\frac{2mT}{\hbar^2}\right)^{3/2} C_{1/2}(\eta)\,. \tag{7}$$

For $\rho > \rho_e$, the degeneracy parameter is zero. Once η is known, it is straightforward to calculate the energy and entropy densities:

$$h_{ni}(\rho, T) = \frac{\hbar^2}{2m}\tau(\rho, T) \tag{8}$$

and

$$s_{ni}(\rho, T) = \frac{5}{3}\frac{\hbar^2}{2m}\frac{\tau(\rho, T)}{T} - \eta\rho \tag{9}$$

where

$$\tau(\rho, T) = \frac{1}{2\pi^2}\left(\frac{2mT}{\hbar^2}\right)^{5/2} C_{3/2}(\eta)\,. \tag{10}$$

For $\rho > \rho_e$, the previous expressions are calculated at the value $\eta = 0$. The remaining $(\rho - \rho_e)/\rho$, i.e. the fraction of particles with zero momentum, does not contribute to h_{ni} nor to s_{ni}.

Once the functional (1) is defined, a complete thermodynamical description of the system can be achieved. In particular, the chemical potential and the pressure are given by

$$\mu(\rho, T) = \eta T + \left(\frac{\partial f_v}{\partial \rho}\right)_T \tag{11}$$

and

$$p(\rho, T) = p_{ni}(\rho, T) + \tfrac{1}{2}b\rho^2 + \tfrac{1}{2}c(1+\gamma)\rho^{2+\gamma}\,. \tag{12}$$

The calculated isotherms for $T = 0, 3, 5$ and 7.4 K (critical isotherm of this model) are presented in figure 3, showing how the stability condition

$$\left(\frac{\partial p}{\partial \rho}\right)_T > 0 \tag{13}$$

is violated over a wide range of densities and temperatures, thus indicating that the system has to split in two phases, a dense one (liquid L) and a dilute one (gas G). At a given T, these phases can be determined by solving the equilibrium conditions:

$$\begin{aligned} \mu_L(\rho_L, T) &= \mu_G(\rho_G, T) \\ p_L(\rho_L, T) &= p_G(\rho_G, T)\,. \end{aligned} \tag{14}$$

This model leads only to a qualitative description of the phase separation. In particular, it yields a critical temperature and pressure of 7.4 K and 4.8 atm respectively, to be compared with the experimental values $T_c = 5.20$ K and $P_c = 2.24$ atm. Recently, a mean field calculation [19] carried out using the results of a path integral Monte Carlo calculation for hard spheres at temperatures above T_λ, yields $T_c = 6.8$ K and $P_c = 4.9$ atm, which are similar to the results we have obtained.

To improve on the thermodynamical description of the ^{4}He liquid–gas system, we take a more phenomenological point of view and make the parameters b and c T-dependent by imposing that at a given temperature, the pressure and the liquid density obtained by solving (14) be the experimental ones [20,21]. The exponent γ has been kept T-independent. This is the procedure we followed in [14] for liquid ^{3}He. The fit has been carried out from $T = 0.5$ K to 5 K with a T-step of 0.05 K. The critical region above 5 K has been left out of the fit because it is beyond the reach of a mean field description. The region below 0.5 K has not been considered, because the ^{4}He vapour is so rare that it would not affect in any appreciable amount the properties of the liquid and its surface. Other methods that put the emphasis in the liquid phase alone are better suited to study the T-dependence of the surface properties in this regime [17,22,23].

The T-dependent functional has to be modified to eliminate the unphysical peak in the specific heat coming from the Bose expression for $f_{ni}(\rho, T)$, which shows up near 3.2 K (small dotted peak in figure 2). This peak is not eliminated by the T-dependence of the b- and c-coefficients. To wash it out, we have further modified the functional, using above $T = 2.8$ K the classical free gas instead of the Bose expression for $f_{ni}(\rho, T)$. This matching temperature can be arbitrarily chosen between T_λ and the spurious peak at ≈ 3.2 K without introducing any appreciable change in the results. From this point on, all the results we shall discuss have been obtained with this modified free energy functional.

Figure 4 shows the coexistence curve. The full circles correspond to the experimental data [20,21] and the full curve to our calculation. The extrapolation of the calculated (up to 5 K) coexistence curve gives a critical temperature (T_c) of 5.4 K whilst the experimental T_c is 5.20 K. Due to the fit procedure, the experimental thermal expansion coefficient of the liquid

$$\alpha = -\frac{1}{\rho}\left(\frac{\partial \rho}{\partial T}\right) \tag{15}$$

calculated along the coexistence curve is well reproduced. Notice that α is a monotonously increasing function of T above T_λ. It has a discontinuity at T_λ, becoming negative below T_λ and again positive below 1.2 K. In this last region, it is so small that it is difficult to measure [20]. All these features are present in the coexistence curve. The T-dependence of the coefficients b and c gives an explicit

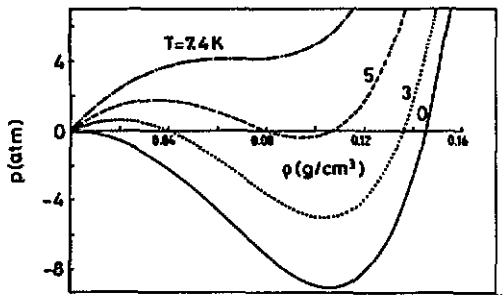

Figure 3. ^{4}He isotherms at different temperatures. The coefficients b and c of the functional are T-independent.

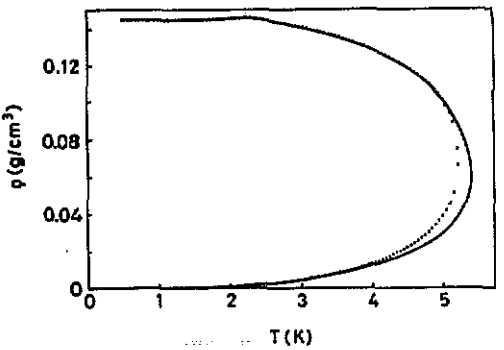

Figure 4. ^{4}He liquid–gas coexistence line. The full circles are the experimental values from [20]. The coefficients b and c are T-dependent (see the text for further explanation).

contribution to quantities like the entropy:

$$s(\rho,T) \equiv s_{ni}(\rho,T) + s_v(\rho,T) = s_{ni}(\rho,T) - \left(\frac{\partial f_v(\rho,T)}{\partial T}\right)_\rho \tag{16}$$

and specific heat,

$$c(\rho,T) = T\left(\frac{\partial s(\rho,T)}{\partial T}\right)_{\rho_L(T)} \tag{17}$$

which is calculated along the coexistence line as indicated by the subscript $\rho_L(T)$ in (17). It is given by:

$$c(\rho,T) = c_{ni}(\rho,T) + T\left(\frac{\partial s_v(\rho,T)}{\partial T}\right)_{\rho_L(T)} \tag{18}$$

where $c_{ni}(\rho,T)$ corresponds to the non-interacting gas contribution. $c(\rho,T)$ (continuous line) is shown in figure 2 together with the experimental results (full circles) [20,21]. From figure 2 one can see that the T-dependence of the coefficients is crucial to reproduce the experimental behaviour of $c(\rho,T)$ around T_λ.

Notice that requiring the functional to reproduce the experimental vapour pressure and the liquid density along the coexistence line implies that the free energy, which can be expressed as

$$f(\rho,T) = -p(\rho,T) + \mu(\rho,T)\rho \tag{19}$$

is also correctly evaluated on the coexistence line when the density of the coexisting gas is low enough to behave as a free classical gas and therefore $\mu_G(\rho,T)$ (thus $\mu_L(\rho,T)$) are correctly given by (14).

Figure 5 shows the $T = 2,3,4$ and 5 K isotherms as well as the calculated (full curve) and experimental (full circles) coexistence curve in the pressure–density plane. Notice that the procedure used to determine $b(T)$ and $c(T)$ consists in

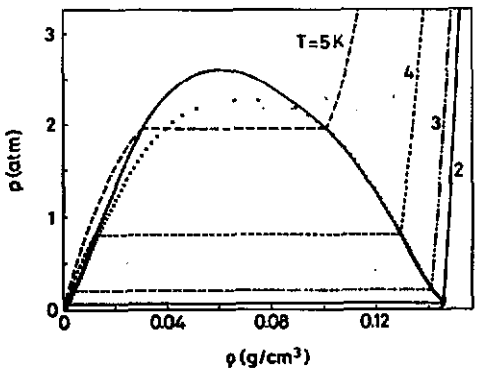

Figure 5. ^{4}He isotherms at different temperatures. The coexistence line in the pressure-density plane is also displayed. The full circles are the experimental values from [20,21].

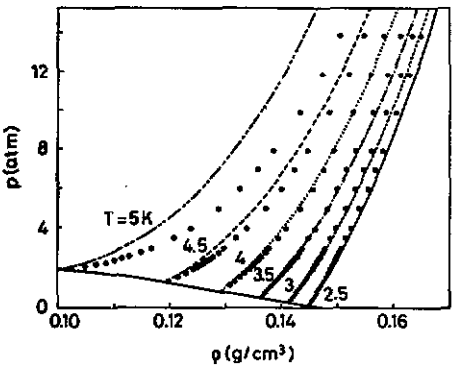

Figure 6. Liquid ^{4}He isotherms at different temperatures above T_λ. The experimental points (full circles) are from [21].

fitting one point along each isotherm, i.e., the crossing point of each isotherm with the liquid branch of the liquid–gas coexistence curve. The discrepancies between the experimental and calculated coexisting vapour densities are an indication of the limitations of the functional. Extrapolating above 5 K the coexistence curve we obtain a critical pressure $P_c = 2.6$ atm whilst the experimental P_c is 2.24 atm.

Figure 6 displays several isotherms corresponding to the liquid phase for temperatures higher than T_λ. The dots are the experimental results [21]. The agreement between the experimental and the calculated isotherms is reasonably good, except for temperatures close to T_c.

3. Liquid–gas interface

3.1. The surface tension

It has been shown in the previous section that the free energy density $F(\rho, T)$, equation (1) is able to describe fairly well the bulk properties of the ^{4}He liquid–gas equilibrium. To study the liquid–gas interface, which is the aim of the present work, $F(\rho, T)$ has to be completed by adding terms which account for density inhomogeneities. The simplest ansatz is to write the free energy per unit volume as:

$$f(\rho, T) = F(\rho, T) + \beta \frac{(\nabla \rho)^2}{\rho} + \xi (\nabla \rho)^2 \tag{20}$$

where $F(\rho, T)$ is the bulk part already discussed, the β-term is the correction to the kinetic energy density, and the ξ-term is the surface correction to the interaction energy, equation (2). Zero temperature functionals similar to (20) have been applied to the study of the surface properties of ^{4}He and ^{3}He liquids [10] and droplets [24] at $T = 0$ K. The extension to finite temperature has been recently carried out for liquid ^{3}He [14].

We have taken for β the value $1/4(\hbar^2/2m)$ as in [10]. The parameter ξ, which is taken T-independent, will be chosen so as to reproduce the ^{4}He surface tension

σ at $T = 0$. After fixing ξ, $\sigma(T)$ is calculated and compared with the experimental values.

The ^{3}He surface tension and the corresponding density profile pertaining to functionals of the kind given by (20) have been derived in detail in [14]. Since for ^{4}He there are no significant changes in the derivation, we will just present here the final expressions. We consider a plane interface separating the liquid and gas phases and take the axis perpendicular to it as the z axis. When z goes to $-\infty$, ρ tends to the liquid density ρ_{in} that at a given T is in thermodynamical equilibrium with a gas of density ρ_{out}, which is the limit of ρ when z goes to $+\infty$. The densities ρ_{in} and ρ_{out} are the solutions of (14).

From the Euler–Lagrange equation

$$\frac{\delta f}{\delta \rho} \equiv \frac{\partial f}{\partial \rho} - \nabla \frac{\partial f}{\partial \nabla \rho} = \mu \tag{21}$$

and after following the procedure indicated in [14], one obtains an equation for the density profile:

$$\rho'(z) = -\left(\frac{\Delta F - \mu \Delta \rho}{\beta/\rho + \xi}\right)^{1/2} \tag{22}$$

where ΔF and $\Delta \rho$ are given by

$$\begin{aligned} \Delta F_{in} &\equiv F(z) - F(\rho_{in}) \\ \Delta \rho_{in} &\equiv \rho(z) - \rho_{in}\,. \end{aligned} \tag{23}$$

Similar definitions hold for ΔF_{out} and $\Delta \rho_{out}$, and either the 'in' or the 'out' expressions can be used in (22). This equation can be integrated numerically, yielding $z(\rho)$ rather than $\rho(z)$. However, the *explicit knowledge of $\rho(z)$ is not necessary to* determine $\sigma(T)$ which can be calculated with the following expression [14]:

$$\sigma(T) = 2\int_{\rho_{out}}^{\rho_{in}} [F(\rho) - F(\rho_{out}) - \mu(\rho - \rho_{out})]^{1/2}\left(\frac{\beta}{\rho} + \xi\right)^{1/2} d\rho\,. \tag{24}$$

We want to emphasize that only bulk quantities are needed to determine $\sigma(T)$, ρ is just the integration variable. When $T = 0$, $\rho_{out} = 0$ and μ becomes the energy *per particle at saturation.*

Taking the experimental value [4] $\sigma = 354.4$ mdyn cm^{-1} at $T = 0$ K, we fix the parameter $\xi = 2047.9$ K Å^5. In [10], the experimental value of reference [2] (378.3 mdyn cm^{-1}) was used, which implies a larger ξ-coefficient, $\xi = 2383$ K Å^5. The T-evolution of the surface tension is shown in figure 7. One can see that the overall agreement between theory (full curve) and experiment (full circles) is rather good. Although the proposed approach is too phenomenological to discuss fine details or to disentangle the contributions of the different types of excitations to the surface energy, we would like to mention that the calculated decrease of the surface tension at small temperature (from 0 to 1 K) is well fitted by $\Delta\sigma(T) = -12.35\ T^{2.33}$ mdyn cm^{-1} while the experimental results adjust to $\Delta\sigma(T) = -7.43\ T^{2.39}$ mdyn cm^{-1}. On the other hand, the ripplon contribution [22] has been estimated to be $\Delta\sigma(T) = -6.50\ T^{7/3}$ mdyn cm^{-1}.

3.2. Surface thickness and density profile

At the liquid–vapour interface, the density $\rho(z)$ smoothly changes from the liquid to the vapour density over a distance of a few ångströms. The surface thickness t gives a quantitative idea of the width of the region where the change occurs. It is defined as $t \equiv z_{in} - z_{out}$, where z_{in} is the point at which $\rho = \rho_{out} + 0.9(\rho_{in} - \rho_{out})$ and z_{out} is the point at which $\rho = \rho_{out} + 0.1(\rho_{in} - \rho_{out})$, ρ_{in} and ρ_{out} being the densities of bulk liquid and vapour in equilibrium.

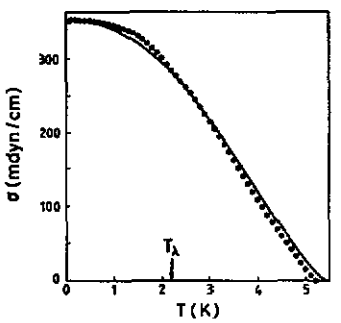

Figure 7. Surface tension as a function of T. The full circles are the experimental values from [4].

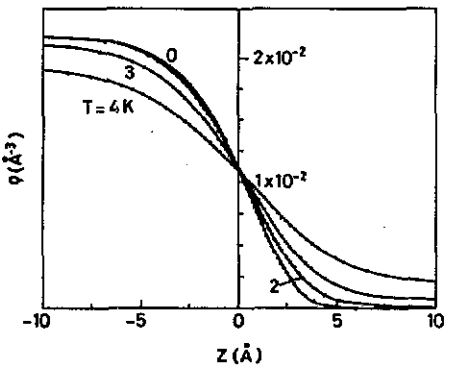

Figure 8. Density profiles at different temperatures. The full circles are the result of a fit of the variational densities to generalized Fermi functions—see equation (25).

Figure 8 shows the $T = 0, 2, 3$ and 4 K density profiles we have obtained integrating equation (22). Each surface has been located around a common $z = 0$ point by imposing that $\rho(0) = \rho_{out} + (\rho_{in} - \rho_{out})/2$. These profiles can be fitted very well by generalized Fermi functions of the kind:

$$\rho(z) = \rho_{out} + \frac{\rho_{in} - \rho_{out}}{[1 + \exp((z - z_0)/\delta)]^\nu} . \tag{25}$$

The full circles along the density profiles in figure 8 are the results obtained using the parametrized densities (25). The surface thickness corresponding to a density of the type given by (25) is readily obtained:

$$t = \delta \ln\left(\frac{10^{1/\nu} - 1}{(10/9)^{1/\nu} - 1}\right) . \tag{26}$$

At low temperatures, the density profiles are very asymmetric around the inflexion point of $\rho(z)$. This is reflected in the value of ν ($\nu = 4.8$ at $T = 0$ K). When T increases, the density profile becomes more symmetric ($\nu = 1.8$ at $T = 3$ K).

From the fully variational density profile we get $t = 6.45$ Å at $T = 0$ K. The difference with the value reported in [10] ($t = 7$ Å) is due to the different values we have used for $\sigma(0)$. The incorporation of finite-range effects in the density-functional points to smaller values of t (5.7 Å in reference [11]). Recent Monte

Carlo and Green's Function Monte Carlo calculations [9] carried out for the Aziz potential also yield a smaller value ($t \approx 5$ Å). Other calculations give values of t from 2 to 11.5 Å (see [6] and references therein). The result for $t(T)$ obtained from the variational densities is shown in figure 9. It can be seen that t changes very little up to 1 K, and around 0.5 Å from 1 to 1.5 K. Above this temperature, t increases rapidly with T.

The density profile has not been experimentally determined so far. In [6], a characteristic length of the liquid–gas interface was deduced from ellipsometric measurements in the temperature range of 1.4 to 2.1 K. This length is defined in the following way [6,25]:

$$\zeta = \int_{-\infty}^{+\infty} \frac{(n^2 - n_{\text{out}}^2)(n^2 - n_{\text{in}}^2)}{n^2} \mathrm{d}z \tag{27}$$

where $n(z)$ is the refractive index at the position z and the integration extends from bulk liquid ($n = n_{\text{in}}$) up through the transition layer into the vapour ($n = n_{\text{out}}$). In the next step, the Lorentz–Lorentz relation between the square of the refractive index, the density and the polarizability [26] was used [6] in conjunction with a simple Fermi function ((25), with $\nu = 1$) to get a relationship between the thickness, the refractive indexes of the liquid and the gas, and the measured quantity ζ. The polarizability was considered constant in the whole density range, which is justified by some experimental evidence [26]. The average thickness determined in reference [6] for T from 1.4 to 2.1 K is 9.36 Å. Extrapolating his results, Osborne [6] predicts $t = 8.5$ Å at $T = 0$ K, thus indicating that the surface thickness has increased 1–2 Å in this temperature interval.

Consequently, the only indirect experimental determination of t carried out so far seems to point towards a value of the surface thickness 2–3 Å larger than the most recent calculations. Since in the analysis of the ellipsometric measurements of reference [6] it was used a symmetric ($\nu = 1$) density profile, it is worth checking if it has some influence on the extracted value of t (our calculations and those of reference [10] yield very asymmetric density profiles). We have verified that this is not the case. Indeed, if instead of the $T = 0$ best fit parameters $\nu = 4.8$, $\delta = 1.97$ Å which yield $t = 6.45$ Å we use $\nu = 1$ and the readjusted value $\delta = 1.47$ Å (which also yields a rather good fit in the surface region) we get $t = 6.44$ Å.

Using (27), we have calculated the quantity ζ as a function of the temperature for different types of profiles. The results are shown in figure 10 in the range of temperatures for which n_{in} and n_{out} are experimentally known [26]. The full curve corresponds to the calculation with the variational profiles obtained from (22); the broken and chain curves correspond to the fitted profiles with $\nu = 1$ and 2, respectively (equation (27) can be analytically integrated for any ν integer).

The non-monotonic behaviour of $\zeta(T)$ can be easily understood as follows. Taking $\nu = 1$ in (25), we get from (26) and (27) (see also reference [6]):

$$t(T) = 4\delta(T) \ln 3$$

$$\zeta(T) = -\delta(T) \left[(n_{\text{out}}^2 - n_{\text{in}}^2) \ln \frac{n_{\text{out}}}{n_{\text{in}}} \right] . \tag{28}$$

The function within brackets is always positive, going to zero when T approaches T_c. At moderated temperatures, the T-dependence of $\zeta(T)$ is basically determined by

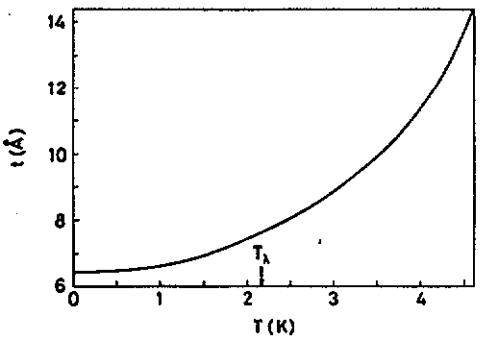

Figure 9. Surface thickness t as a function of T.

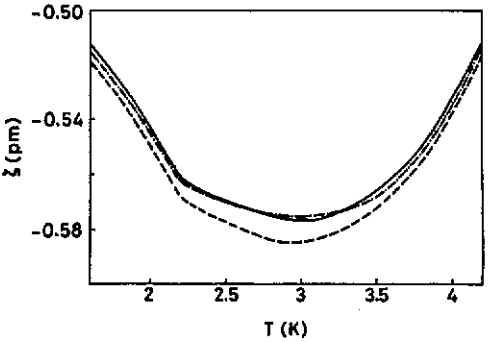

Figure 10. Temperature dependence of the length ζ (in picometres) calculated with different profiles. Full curve, from the solution of equation (22); broken curve, from (25) with $\nu = 1$, chain curve, with $\nu = 2$.

$\delta(T)$ and thus $\zeta(T)$ decreases. At higher temperatures, the second factor in (28) takes over $\delta(T)$ causing $\zeta(T)$ to increase and eventually become zero at T_c.

The average absolute values of the measured ζ ($\zeta \approx -0.7$ pm in the temperature interval $1.4\ \text{K} < T < 2\ \text{K}$) are larger than the calculated ones. Due to the large scale used in figure 10, they are located out of the frame. One can see from figure 10 that the differences between the values of ζ obtained from the different density profiles are not significant, showing that ζ cannot give any reliable information about the surface skewness.

4. Summary

We have studied the thermal properties of the ^{4}He free surface. To this end, we have constructed a phenomenological free energy density able to give a fair account of the bulk properties of the ^{4}He liquid–gas equilibrium, especially of the surface tension.

The T-dependence of the density profiles, and in particular of the surface thickness t, has been predicted and discussed. At zero temperature, our calculation yields a thickness that agrees rather well with other microscopic and finite-range density functional approaches [9–11]. Compared with the only indirect experimental determination [6] of t, the more recent theoretical calculations yield values 2–3 Å smaller. However, as it is mentioned in [6], the experimental accuracy has to be improved before drawing any definitive conclusion.

Our calculations indicate that a sizeable change in the surface thickness occurs only for temperatures above $T \approx 1.5$ K. In this sense, it is highly desirable to have experimental measurements of t above T_λ, for which our calculations may give a first estimate.

Finally, we believe that the present density functional method, as well as that of reference [14], can provide a convenient starting point to study the properties of He droplets at finite T. Calculations in this direction are presently in progress.

Acknowledgments

We would like to thank Professors D V Osborne and M Silbert for their useful

correspondence. This work has been supported by DGICYT (Spain) Grant No. PB89-0332.

References

[1] van Urk A T, Keesom W H and Kamerlingh Onnes H 1925 *Proc. R. Akad. Sci. Amsterdam* **28** 958
[2] Edwards D O and Saam W F 1978 *Prog. Low Temp. Phys.* A **7** 283
[3] Guo H M, Edwards D O, Sarwinski R E and Tough J T 1971 *Phys. Rev. Lett.* **27** 1259
[4] Iino M, Suzuki M and Ikushima A J 1985 *J. Low Temp. Phys.* **61** 155
[5] Echenique P M and Pendry J B 1976 *Phys. Rev. Lett.* **37** 561
[6] Osborne D V 1989 *J. Phys.: Condens. Matter* **1** 289
[7] Saarela M, Pietilainen P and Kallio A 1983 *Phys. Rev.* B **27** 231
[8] Krotscheck E, Qian G X and Kohn W 1985 *Phys. Rev.* B **31** 4245
[9] Vallés J L and Schmidt K E 1988 *Phys. Rev.* B **38** 2879
[10] Stringari S and Treiner J 1987 *Phys. Rev.* B **36** 8369
[11] Dupont-Roc J, Himbert M, Pavloff N and Treiner J 1990 *J. Low Temp. Phys.* **81** 31
[12] Stringari S 1988 *Proc. Int. School Phys. Enrico Fermi CVII Course (Varenna, Italy)*
[13] Stringari S, Barranco M, Polls A, Nacher P J and Laloe F 1987 *J. Physique* **48** 911
[14] Barranco M, Pi M, Polls A and Vinas X 1990 *J. Low Temp. Phys.* **80** 77
[15] Campbell C E, Kurten K E, Ristig M L and Senger G 1984 *Phys. Rev.* B **30** 3728
[16] Ceperley D and Pollock E L 1986 *Phys. Rev. Lett.* **56** 351
[17] Dalfovo F and Stringari S 1989 *J. Low Temp. Phys.* **77** 307
[18] Pathria R K 1972 *Statistical Mechanics* (Oxford: Pergamon) ch 7
[19] Runge K J and Chester G V 1989 *Phys. Rev.* B **39** 2707
[20] Wilks J 1967 *Properties of Liquid and Solid Helium* (Oxford: Clarendon)
[21] McCarty R D 1973 *J. Phys. Chem. Ref. Data* **2** 924
[22] Atkins K R 1953 *Can. J. Phys.* **31** 1165
[23] Salvino R E 1989 *J. Low Temp. Phys.* **76** 121
[24] Stringari S and Treiner J 1987 *J. Chem. Phys.* **87** 5021
[25] Drude P 1959 *Theory of Optics* (New York: Dover) (first published in 1900)
[26] Edwards M H 1957 *Phys. Rev.* **108** 1243; 1958 *Can. J. Phys.* **36** 884